FEBS Letters 412 (1997) 388–396 FEBS 18812

Crystal structure of tetranectin, a trimeric plasminogen-binding protein with an α-helical coiled coil

Bettina Bryde Nielsen[a,*], Jette Sandholm Kastrup[a], Hanne Rasmussen[a], Thor Las Holtet[b], Jonas Heilskov Graversen[b], Michael Etzerodt[b], Hans Christian Thøgersen[b], Ingrid Kjøller Larsen[a]

[a]*Department of Medicinal Chemistry, Royal Danish School of Pharmacy, DK-2100 Copenhagen, Denmark*
[b]*Laboratory of Gene Expression, Department of Molecular and Structural Biology, University of Aarhus, DK-8000 Aarhus C, Denmark*

Received 20 May 1997

Abstract Tetranectin is a plasminogen kringle 4-binding protein. The crystal structure has been determined at 2.8 Å resolution using molecular replacement. Human tetranectin is a homotrimer forming a triple α-helical coiled coil. Each monomer consists of a carbohydrate recognition domain (CRD) connected to a long α-helix. Tetranectin has been classified in a distinct group of the C-type lectin superfamily but has structural similarity to the proteins in the group of collectins. Tetranectin has three intramolecular disulfide bridges. Two of these are conserved in the C-type lectin superfamily, whereas the third is present only in long-form CRDs. Tetranectin represents the first structure of a long-form CRD with intact calcium-binding sites. In tetranectin, the third disulfide bridge tethers the CRD to the long helix in the coiled coil. The trimerization of tetranectin as well as the fixation of the CRDs relative to the helices in the coiled coil indicate a demand for high specificity in the recognition and binding of ligands.

Key words: C-type lectin; X-ray crystal structure; Carbohydrate recognition domain; Plasminogen; Kringle 4; α-Helical coiled coil

1. Introduction

Tetranectin (TN), originally isolated from human plasma [1], is abundant in a variety of cells, including monocytes [2], neutrophils [3], fibroblasts [4], and osteoblasts [5]. The tissue distribution of TN is broad [6] and, in addition, TN is present in the extracellular matrix of certain human carcinomas (breast [7], colonic [8], and ovarian [9] tumors) contrary to the corresponding normal tissues [6]. TN has been shown to bind specifically to the kringle 4 domain of plasminogen (apparent $K_d = 0.5$ μM) [1,10]. In addition, TN interacts in a calcium-dependent manner with sulfated polysaccharides [11] and fibrin [12], as well as with apolipoprotein(a) [10]. The plasminogen activation system is of key importance for regulation and control of extracellular proteolysis and consequently in the spread of cancer by invasion [13,14]. Recently, TN has been co-localized with plasminogen/plasmin at the invasive front of cutaneous melanoma lesions [15], indicating a coordinated role of these proteins in the invasive process. TN may also play a potential role in mineralization during osteogenesis [5,16].

Human TN is a homotrimeric protein [17], each polypeptide chain consisting of 181 amino acid residues encoded by three exons [18]. TN contains a carbohydrate recognition domain (CRD) and, according to sequence homology studies, belongs to a distinct group of the C-type (calcium dependent) lectin superfamily, which also includes pancreatic stone protein (lithostathine), sea raven antifreeze protein, and snake venom botrocetin, all isolated CRDs without additional domains in contrast to TN [19,20]. The X-ray structure of human lithostathine, which is a C-type lectin homolog without calcium-binding sites, has recently been published [21]. In addition, structure determinations of proteins of two other groups of C-type lectins have been reported: the group of collectins (three mannose-binding proteins, rat MBP from serum (MBP-A), rat MBP from liver (MBP-C), human MBP) [22–26], and of selectins (human E-selectin) [27].

We present here the X-ray structure of recombinant human TN. Knowledge on the structure of TN is essential for unraveling the molecular mechanisms of action determining the biological functions of this protein and for the development of drugs interfering with its function.

2. Materials and methods

Rhombohedral crystals belonging to space group R3, with hexagonal axes $\mathbf{a} = \mathbf{b} = 89.1$, and $\mathbf{c} = 75.8$ Å have been obtained of TN. Diffraction data have been collected to 2.8 Å resolution, and a molecular replacement solution, using the CRD of rat MBP from serum, has been obtained [28]. A partially refined structure (2.0 Å resolution) of the CRD of TN, which have been crystallized separately [28], was subjected to a slow-cool protocol refinement in X-PLOR [29] using diffraction data in the resolution range 10.0–3.2 Å. In addition to the CRD, one turn of an α-helix preceding the CRD could be located in the initial electron density maps (25.0–3.2 Å), and was inserted as polyalanine residues. Then interactive model building and refinements using the molecular graphics program O [30] and the refinement program TNT [31,32], respectively, gradually improved the maps, and turn by turn of the α-helix could be located. Side chains were included as they appeared in the electron density maps. Refinements and map calculations in TNT were performed using data in the resolution range 25.0–2.8 Å. The final refinements were done using the positional refinement implemented in X-PLOR and data in the resolution range 6.0–2.8 Å and a cutoff of 2.5σ. Two calcium ions, as well as 36 water molecules, were located in difference Fourier maps (3σ). The positions of the calcium ions were kept constant during refinements. The B-factors were kept constant at 25 Å^2 for protein atoms and calcium ions, and at 40 Å^2 for water molecules. The final statistics are shown in Table 1. The coordinates have been deposited in the Brookhaven Protein Data Bank.

*Corresponding author. Fax: (45) 3537-2209.
E-mail: bettina@medchem.dfh.dk

PII S0014-5793(97)00664-9

3. Results and discussion

3.1. Overall structure

The structure of TN has been determined to 2.8 Å resolution and refined to an *R*-value of 22.3% (Table 1). The protein crystallizes as a trimer in agreement with the observations in solution [17]. The residues 26–181 of TN are clearly defined in the electron density maps. The N-terminal 25 residues can not be located in the electron density maps, indicating disorder in the N-terminal part of TN.

The residues 26–52 of TN form a long α-helix (E2), which is connected to the CRD (res. 50–181) (Fig. 1a). The CRD of TN has the same characteristic topology as reported for the other proteins of the C-type lectin superfamily [21–27]. Structural differences mainly occur at insertions and deletions in TN as compared to human lithostathine [21], human MBP [26], and human E-selectin [27] (Table 2 and Fig. 1b). Two calcium ions have been located at the same positions as calcium-binding sites 1 and 2 in the structures of the MBPs [22–26]. In TN, the ligands are Asp^{116}, Glu^{120}, Gly^{147}, Glu^{150}, and Asn^{151} at calcium site 1 and Gln^{143}, Asp^{145}, Glu^{150}, and Asp^{165} at calcium site 2. TN, as well as lithostathine, contains a long-form CRD with three disulfide bridges in contrast to the MBPs and E-selectin, which have short-form CRDs with two disulfide bridges [19]. In TN, the disulfide bridge Cys^{50}–Cys^{60} tethers the E2 helix to a short β-strand of the CRD (Fig. 1a), whereas this disulfide bridge is part of a loop in lithostathine [21] (Fig. 1b). The CRD of TN has been crystallized separately [28]. The detailed structure (2.0 Å resolution) of the CRD has been fully refined and will be reported elsewhere.

3.2. Trimerization through a coiled coil

The long E2 helix provides trimerization of TN by the formation of a triple α-helical coiled coil (Fig. 1c,d). Only few contacts are observed among the CRDs of the trimer, in agreement with the observation that the isolated CRD of TN is a monomer in solution [17]. The first 16 N-terminal residues of TN are not essential for the trimerization as the polypeptide TN17-181, which have been expressed separately, also forms trimers in solution [17] as well as in crystals (Nielsen, B.B., unpublished).

The main interactions among TN monomers are localized to the core of the triple α-helical coiled coil (Fig. 2a). The amino acid sequence of the E2 helix is characterized by the heptad repeats $(abcdefg)_n$ with hydrophobic amino acids at **a** and **d** positions as are other α-helical coiled coils [33]. Notably, the polar residues Gln^{44} and Gln^{47} substitute the usual hydrophobic residues at the **a** and **d** positions in the C-terminal repeat. The side chain of Gln^{44} is pointing out, leaving a hole in the helix core, and forms a hydrogen bond to the side chain of Gln^{43} of a neighboring E2 helix, whereas the side chain of Gln^{47} is pointing into the core.

The presence of hydrophobic β-branched residues at **a** and **d** positions in the helices of coiled coils appears to favor trimerization of the protein [34,35]. Val^{37} is the only relevant β-branched residue in the E2 sequence. Buried polar residues at **a** and **d** positions, however, have been shown to influence the state of oligomerization of the helices [36–38]. The presence of glutamine residues at both an **a** and a **d** position in the repeats, as well as the single valine in an **a** position, may govern trimerization of TN.

3.3. Helix–CRD interactions

In addition to the large interaction area in the α-helical coiled coil, intramolecular interactions between the E2 helix and the N- and C-terminal part of the CRD contribute to the integrity of the trimer. The interactions involve the C-terminal part of the helix where the hydrophobic residues Leu^{46} and Val^{49} are positioned at the outside of the helix. The side chains of these residues are in van der Waals distance to the side chains of Phe^{178}, Ile^{180}, and Val^{181} in the C-terminus of the CRD. The Cβ atom of Lys^{52} in the helix is in van der Waals contact to the side chain of Leu^{62}. These intramolecular interactions, and the disulfide bridge between the CRD and the helix, seem to determine the orientation of the CRD relative to the E2 helix.

3.4. Biological role of TN

The trimeric structure of TN resembles those of rat MBP from serum [25] and human MBP [26], in which the neck region forms a long α-helix. Like TN, the MBPs trimerize by the formation of an α-helical coiled coil. The structural differences are reflected in significantly different orientations of the CRDs relative to the helices as illustrated in Fig. 2b–d, in which the three structures have been superimposed according to the structures of the coiled coils and the heptad repeat sequences (Table 2). The orientations of the CRDs are determined by the coiled coil structure, by intramolecular interactions between the helix and its CRD, and also by intermolecular interactions between each of the helices of the coiled coil and a neighboring CRD.

An important function of the coiled coil in the MBPs is considered to be the relative positioning of the CRDs. The orientation of the CRDs with respect to the coiled coil stem determines the spatial separation of the carbohydrate-binding sites (calcium sites 2), suggesting the function to be recognition of spatially distinct regions on the bacterial cell walls [25,26]. Despite the very different orientations of the CRDs with respect to the coiled coil helices in the monomers of TN, rat MBP, and human MBP (Fig. 2d), the overall shape of the trimers is similar (Fig. 2b–c). However, significant variations

Table 1
Statistics of data and refinement

Space group	R3
Unit cell parameters	**a** = **b** = 89.1 Å, **c** = 75.8 Å (hexagonal axes)
Completeness (25.0–2.8 Å)	99.9%
Completeness (2.87–2.80 Å)	100.0%
Multiplicity (25.0–2.8 Å)	5.5
R_{merge}(I) (25.0–2.8 Å)	10.7%
R_{merge}(I) (3.13–3.03 Å)	29.4%
R_{merge} (I) (2.87–2.80Å)	51.9%
$<I/\sigma(I)>$ (25.0–2.8 Å)	6.7
$<I/\sigma(I)>$ (3.13–3.03 Å)	2.6
$<I/\sigma(I)>$ (2.87–2.80 Å)	1.5
Unique reflections	5529
Total number of atoms	1250
R_{factor} (6.0–2.8 Å)[a]	22.3%
R_{free} (6.0–2.8 Å)[b]	29.2%
	r.m.s. deviations from idealized geometries
Bond lengths (Å)	0.012
Bond angles (°)	1.6
Dihedral angles (°)	24.0

[a] $R_{factor} = \Sigma \mid |F_{obs}| - |F_{calc}| \mid / \Sigma |F_{obs}|$.
[b] R_{free}:R_{factor} of test set containing a random 10% of the observations omitted from the refinement process.

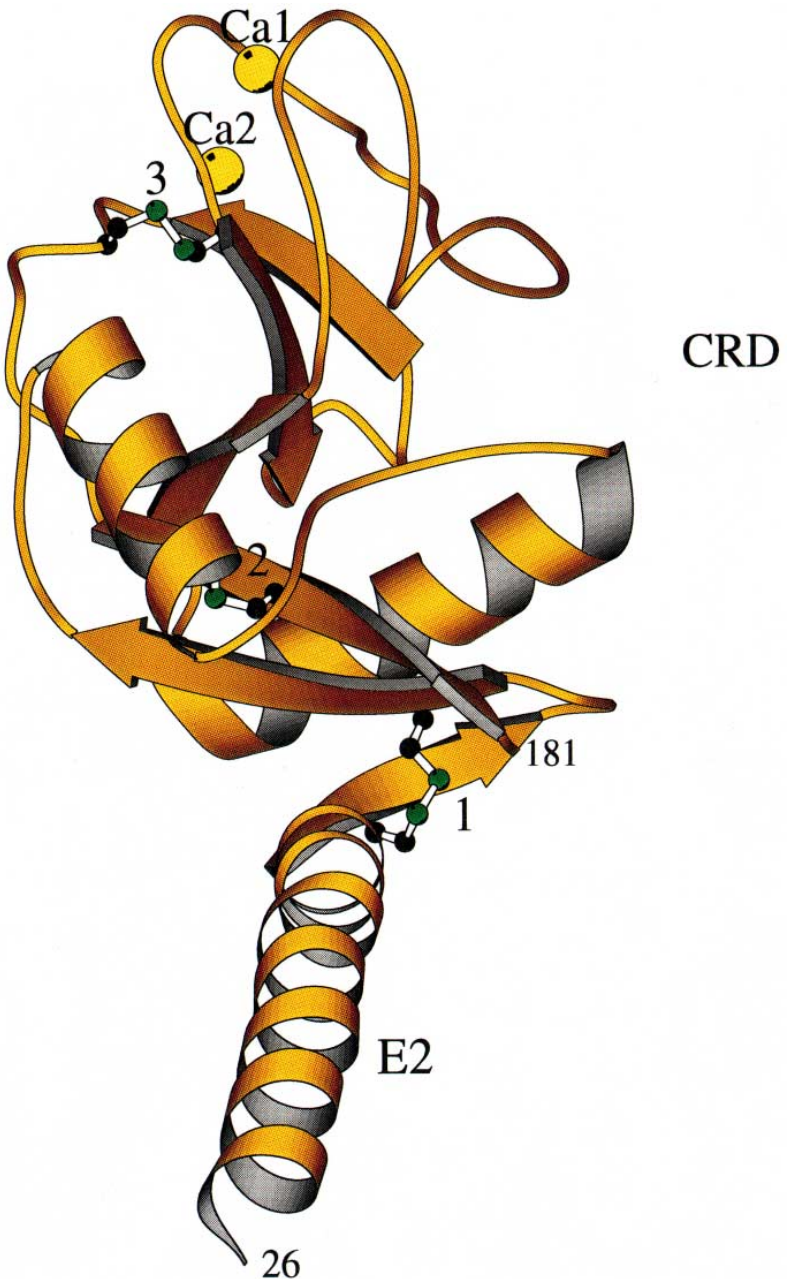

Fig. 1. a: Overall structure of the TN monomer. TN consists of a long α-helix (E2) and a carbohydrate recognition domain (CRD). The two calcium ions are illustrated as yellow spheres, and the three disulfide bridges: 1 (Cys^{50}-Cys^{60}), 2 (Cys^{77}-Cys^{176}), and 3 (Cys^{152}-Cys^{168}), are shown in a ball and stick representation. b: Superposition of the CRDs of human TN (in yellow), human lithostathine (in blue), human MBP (in green), and human E-selectin (in orange). Calcium ions at site 1 and 2 are illustrated as spheres, and the three disulfide bridges in ball and stick. The r.m.s. deviation between TN and lithostathine is 1.5 Å (for 116 Cα atoms), between TN and human MBP 1.2 Å (for 117 Cα atoms), and between TN and human E-selectin 1.3 Å (for 104 Cα atoms). c-d: The overall structure of the TN trimer viewed (c) along and (d) perpendicular to the 3-fold axis. The figures were generated using MOLSCRIPT [39].

in the distances between the calcium sites 2 in the trimeric structures are observed. The distance between the calcium sites 2 in TN is approximately 55 Å. The distances observed in rat MBP and in human MBP are 53 Å and 45 Å, respectively [25,26]. These variations might be of importance for the specificity of the proteins.

The precise biological function of TN is as yet unclear. However, the observations that TN binds to the kringle 4 domain of plasminogen [1,10], interacts in a calcium-dependent manner with sulfated polysaccharides [11] and fibrin [12], binds to immobilized fucoidan (Graversen, J.H., unpublished), as well as the presence of two characteristic calcium sites in the TN structure, suggest that one function of the protein is to target plasminogen to specific carbohydrate ligands on cell surfaces, in the extracellular matrix or to fibrin. The close structural resemblance of TN to the neck and CRD part of the MBPs, where carbohydrate-binding is conferred to the CRD, whereas other additional domains provide the diversity of functions of these proteins, indicate that the kringle 4-binding site resides within residues 1–49 of the TN

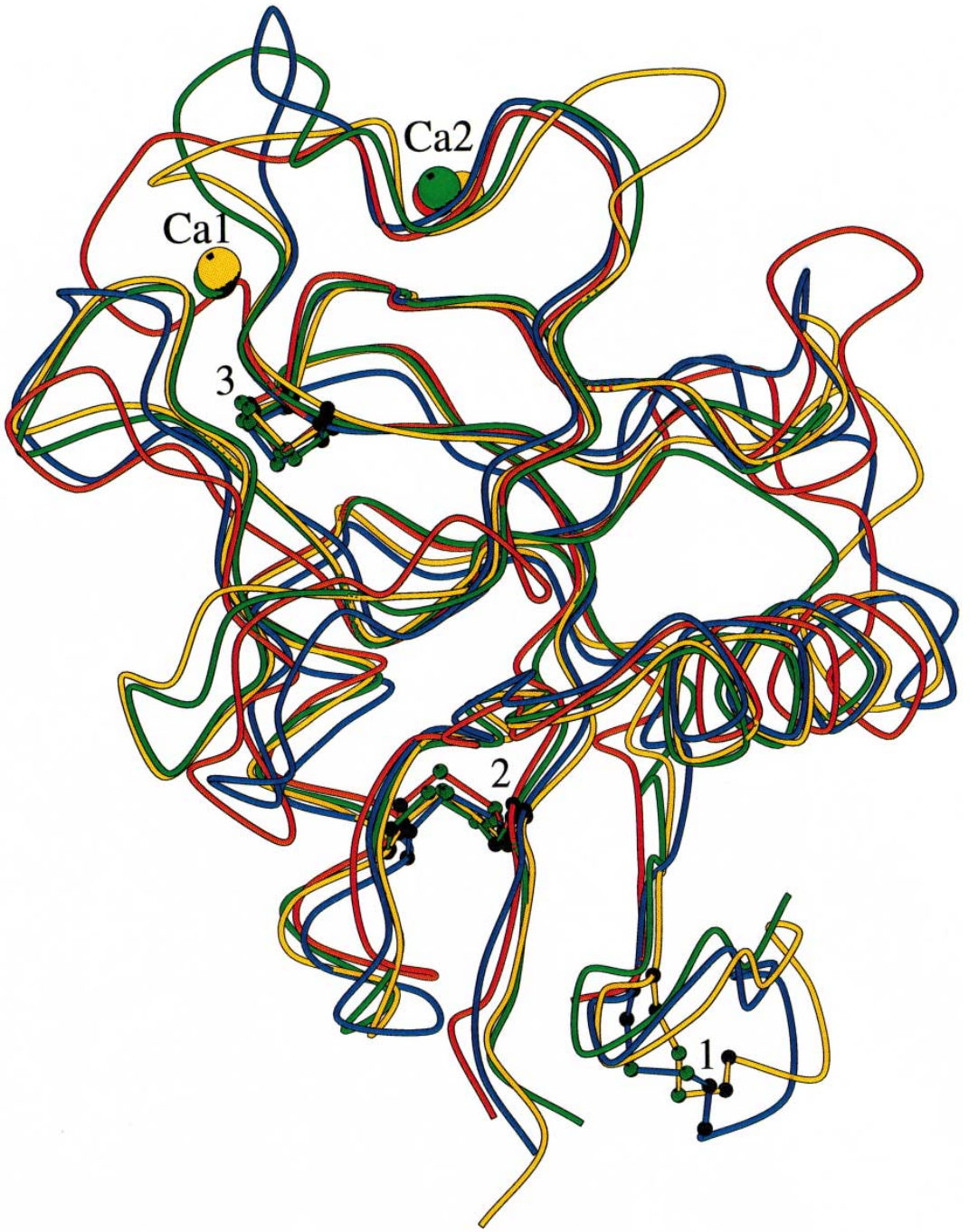

Fig. 1b (for caption see page 390).

sequence. This is supported by the observation that only the full-length protein and not the isolated CRD binds to immobilized kringle 4 (Holtet, T.L., unpublished).

The additional disulfide bridge in TN, which is not present in the human MBP and rat MBP, seems to tether the CRD to the helix, and prevents flexibility of the CRD relative to the helix. In human MBP, the relative orientation between the CRD and the helix has been shown to be variable, and flexibility of the CRDs has been proposed to be important for cooperative binding of carbohydrates on the target [26]. The fixation of the CRDs in TN indicates a demand for high specificity in recognition and binding of ligands.

Acknowledgements: The technical assistance of Brian Rosenberg is gratefully acknowledged. This work was supported by grants from the Danish Biotechnology Programme, The Lundbeck Foundation, and The EU Network Programme on Protein Crystallography.

References

[1] Clemmensen, I., Petersen, L.C. and Kluft, C. (1986) Eur. J. Biochem. 156, 327–333.

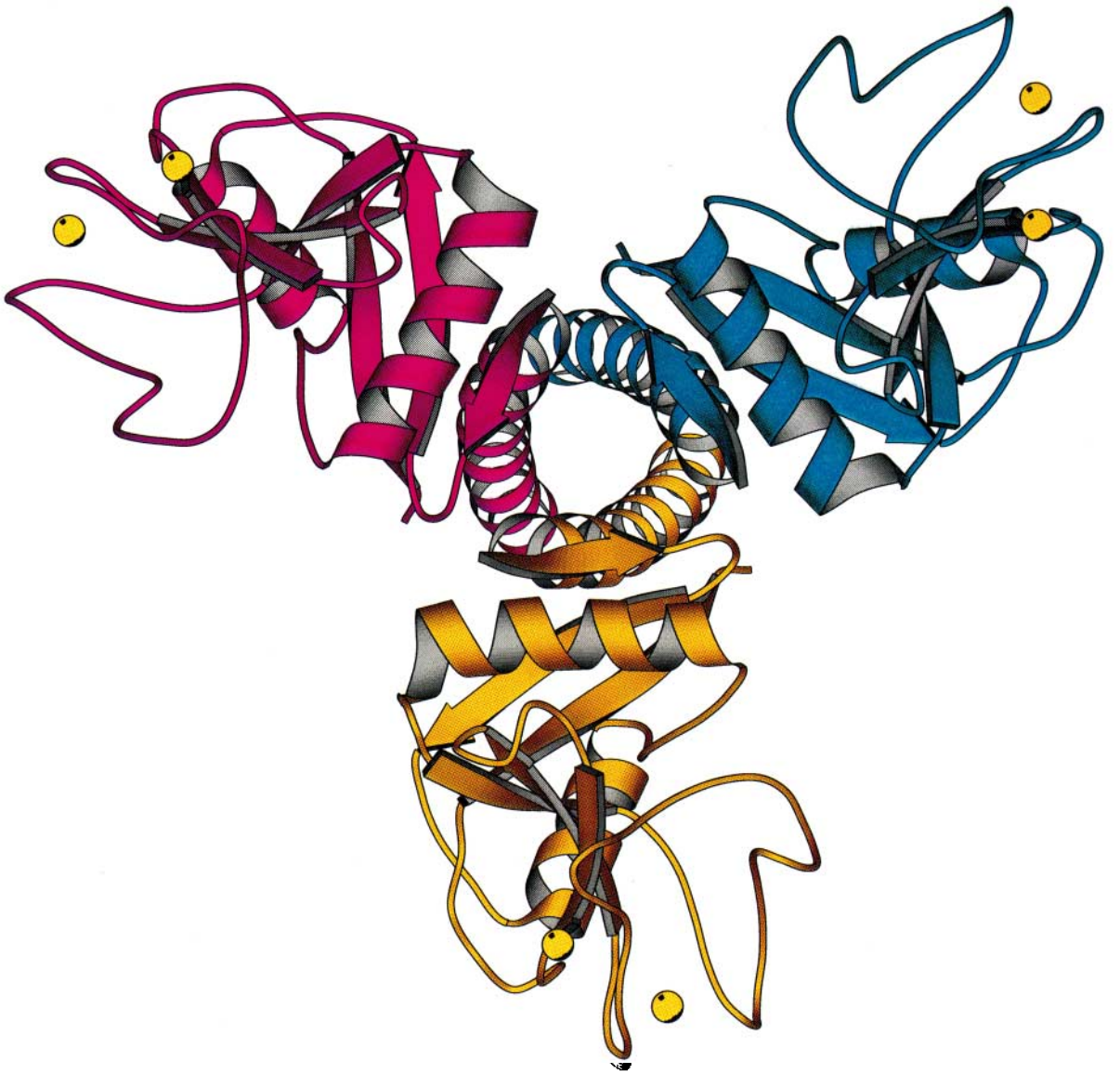

Fig. 1c (for caption see page 390).

[2] Nielsen, H., Clemmensen, I. and Kharazmi, A. (1993) Scand. J. Immunol. 37, 39–42.
[3] Borregaard, N., Christensen, L., Bjerrum, O.W., Birgens, H.S. and Clemmensen, I. (1990) J. Clin. Invest. 85, 408–416.
[4] Clemmensen, I., Lund, L.R., Christensen, L. and Andreasen, P.A. (1991) Eur. J. Biochem. 195, 735–741.
[5] Wewer, U.M., Ibaraki, K., Schjørring, P., Durkin, M.E., Young, M.F. and Albrechtsen, R. (1994) J. Cell Biol. 127, 1767–1775.
[6] Christensen, L. and Clemmensen, I. (1989) Histochemistry 92, 29–35.
[7] Christensen, L. and Clemmensen, I. (1991) Histochemistry 95, 427–433.
[8] Wewer, U.M. and Albrechtsen, R. (1992) Lab. Invest. 67, 253–262.
[9] Høgdall, C.K., Christensen, L. and Clemmensen, I. (1993) Cancer 72, 2415–2422.
[10] Kluft, C., Jie, A.F.H., Los, P., de Witt, E. and Havekes, L. (1989) Biochem. Biophys. Res. Commun. 161, 427–433.
[11] Clemmensen, I. (1989) Scand. J. Clin. Lab. Invest. 49, 719–725.
[12] Kluft, C., Los, P. and Clemmensen, I. (1989) Thromb. Res. 55, 233–238.
[13] Carmeliet, P., Schoonjans, L., Kieckens, L., Ream, B., Degen, J., Bronson, R., De Vos, R., van den Oord, J.J., Collen, D. and Mulligan, R.C. (1994) Nature (Lond.) 368, 419–424.
[14] Danø, K., Behrendt, N., Brünner, N., Ellis, V., Ploug, M. and Pyke, C. (1994) Fibrinolysis 8, 189–203.
[15] De Vries, T.J., De Wit, P.E.J., Clemmensen, I., Verspaget, H.W., Weidle, U.H., Bröcker, E.B., Ruiter, D.J. and Van Muijen, G.N.P. (1996) J. Pathol. 179, 260–265.
[16] Iba, K., Sawada, N., Chiba, H., Wewer, U.M., Ishii, S. and Mori, M. (1995) FEBS Lett. 373, 1–4.
[17] T.L. Holtet, J.H. Graversen, H.C. Thøgersen, I. Clemmensen, M. Etzerodt, Protein Sci. in press.
[18] Berglund, L. and Petersen, T.E. (1992) FEBS Lett. 309, 15–19.
[19] Day, A.J. (1994) Biochem. Soc. Trans. 22, 83–87.
[20] Drickamer, K. and Taylor, M.E. (1993) Annu. Rev. Cell Biol. 9, 237–264.
[21] Bertrand, J.A., Pignol, D., Bernard, J.-P., Verdier, J.-M., Dagorn, J.-C. and Fontecilla-Camps, J.C. (1996) EMBO J. 15, 2678–2684.
[22] Weis, W.I., Kahn, R., Fourme, R., Drickamer, K. and Hendrickson, W.A. (1991) Science 254, 1608–1615.
[23] Weis, W.I., Drickamer, K. and Hendrickson, W.A. (1992) Nature 360, 127–134.

Fig. 1d (for caption see page 390).

[24] Ng, K.K.-S., Drickamer, K. and Weis, W.I. (1996) J. Biol. Chem. 271, 663–674.
[25] Weis, W.I. and Drickamer, K. (1994) Structure 2, 1227–1240.
[26] Sheriff, S., Chang, C.Y. and Ezekowitz, R.A.B. (1994) Nat. Struct. Biol. 1, 789–794.
[27] Graves, B.J., Crowther, R.L., Chandran, C., Rumberger, J.M., Li, S., Huang, K.-S., Presky, D.H., Familletti, P.C., Wolitzky, B.A. and Burns, D.K. (1994) Nature (Lond.) 367, 532–538.
[28] Kastrup, J.S., Rasmussen, H., Nielsen, B.B., Larsen, I.K., Holtet, T.L., Graversen, J.H., Etzerodt, M. and Thøgersen, H.C. (1997) Acta Crystallogr. D53, 108–111.
[29] Brünger, A.T., Kuriyan, J. and Karplus, M. (1987) Science 235, 458–460.
[30] Jones, T.A., Zou, J.-Y., Cowan, S.W. and Kjeldgaard, M. (1991) Acta Crystallogr. A47, 110–119.
[31] Tronrud, D.E., Ten Eyck, L.F. and Mattews, B.W. (1987) Acta Crystallogr. A43, 489–501.
[32] Tronrud, D.E. (1992) Acta Crystallogr. A48, 912–916.
[33] Lupas, A. (1996) TIBS 21, 375–382.
[34] Harbury, P.B., Zhang, T., Kim, P.S. and Alber, T. (1993) Science 262, 1401–1407.
[35] Harbury, P.B., Kim, P.S. and Alber, T. (1994) Nature (Lond.) 371, 80–83.
[36] Lumb, K.J. and Kim, P.S. (1995) Biochemistry 34, 8642–8648.
[37] Gonzalez Jr., L., Brown, R.A., Richardson, D. and Alber, T. (1996) Nature Struct. Biol. 3, 1002–1010.
[38] Gonzalez Jr., L., Woolfson, D.N. and Alber, T. (1996) Nat. Struct. Biol. 3, 1011–1018.
[39] Kraulis, P.J. (1991) J. Appl. Cryst. 24, 946–950.

Table 2

Alignment of the amino acid sequences of human TN (TN), human MBP (hMBP), rat MBP from serum (rMBP, the neck and CRD part), human E-selectin (the CRD part), and human lithostathine (hlit).

The sequences were aligned according to 3-dimensional structural similarities. Residues, which have not been located in the crystal structures, are colored in grey, residues of the CRDs are colored in red, and remaining residues in blue. Secondary structure elements and loop regions of TN are indicated and labelled according to the structures of the MBPs.

```
                1                 10                  20                    30
TN secondary structure                                              | - - - - - E2 helix - - - - - -
TN              G E P P T Q K P K K I V N A K K D V V N T K M F E E L K S R L D T L S Q E V A
hMBP                                                            P D G D S S L A - - A S E R K
rMBP                                                              A I E V K L A N M E A E I N
Heptad repeat                                                       d e f g a b c d e f g a b
E-selectin
hlit                                                                                      Q E

                  40                  50                          60                  70
                - - - - - - E2 helix - - - | | - - β0 - -|     | - - β1 - - |      | - - α1 - - -
TN              L L K E Q Q A L Q T V C - L K G - - - T K V H M K C F L A F T Q T K T F H E A
hMBP            A L Q T E M A R I K K W - L T F S L G K Q V G N K F F L T N G E I M T F E K V
rMBP            T L K S K L E L T N K L - H A F S M G K K S G K K F F V T N H E R M P F S K V
Heptad repeat   c d e f g a b c d e f g   a
E-selectin                                                      W S Y N T S T E A M T Y D E A
hlit            A Q T E L P Q A R I S C P E G T - - - N A Y R S Y C Y Y F N E D R E T W V D A

                            80                    90                  100                 110
                - - α1 - - |                   | - - - - - - - α2 - - - - - - -|     | - β2 - -
TN              S E D C I S R - G G T L S T P Q T G S E N D A L Y E Y L R Q S V G N E A E I W
hMBP            K A L C V K F - Q A S V A T P R N A A E N G A I Q N L I K - - - - - - E E A F
rMBP            K A L C S E L - R G T V A I P R N A E E N K A I Q E V A K - - - - - - T S A F
E-selectin      S A Y C Q Q R - Y T H L V A I Q N K E E I E Y L N S I L S Y S P - - - S Y Y W
hlit            D L Y C Q N M N S G N L V S V L T Q A E G A F V A S L I K E S G T D D F N V W

                                120                   130                     140
                - |    | - - - L1 - -|   | - - L2 - |              | - - - L3 - - - |  | - L4 -
TN              L G L N D M A A E G T W V D M - T G A R I A - - Y K N W E T E I T A Q P D G -
hMBP            L G I T D E K T E G Q F V D L - T G N R L T - - Y T N W N - - - E G E P N N A
rMBP            L G I T D E V T E G Q F M Y V - T G G R L T - - Y S N W K - - - K D E P N D H
E-selectin      I G I R K - V N - N V W V W V G T Q K P L T E E A K N W A - - - P G E P N N R
hlit            I G L H D P K K N R R W H W S S G S L - V S - - Y K S W G - - - I G A P S S V

                      150                       160                   170                 180
                - L4 - - | | - β3 - |              | - β4 -|             | - - - β5 - - -|
TN              G K T E N C A V L S G A - - - A N - G K W F D K R C R D Q L P Y I C Q F G I V
hMBP            G S D E D C V L L L K - - - - - N - G Q W N D V P C S T S H L A V C E F P I
rMBP            G S G E D C V T I V D - - - - - N - G L W N D I S C Q A S H T A V C E F P A
E-selectin      Q K D E D C V E I Y I K R E K D V - G M W N D E R C S K K K L A L C Y T A A
hlit            N - P G Y C V S L T S S - - - T G F Q K W K D V P C E D K F S F V C K F K N
```

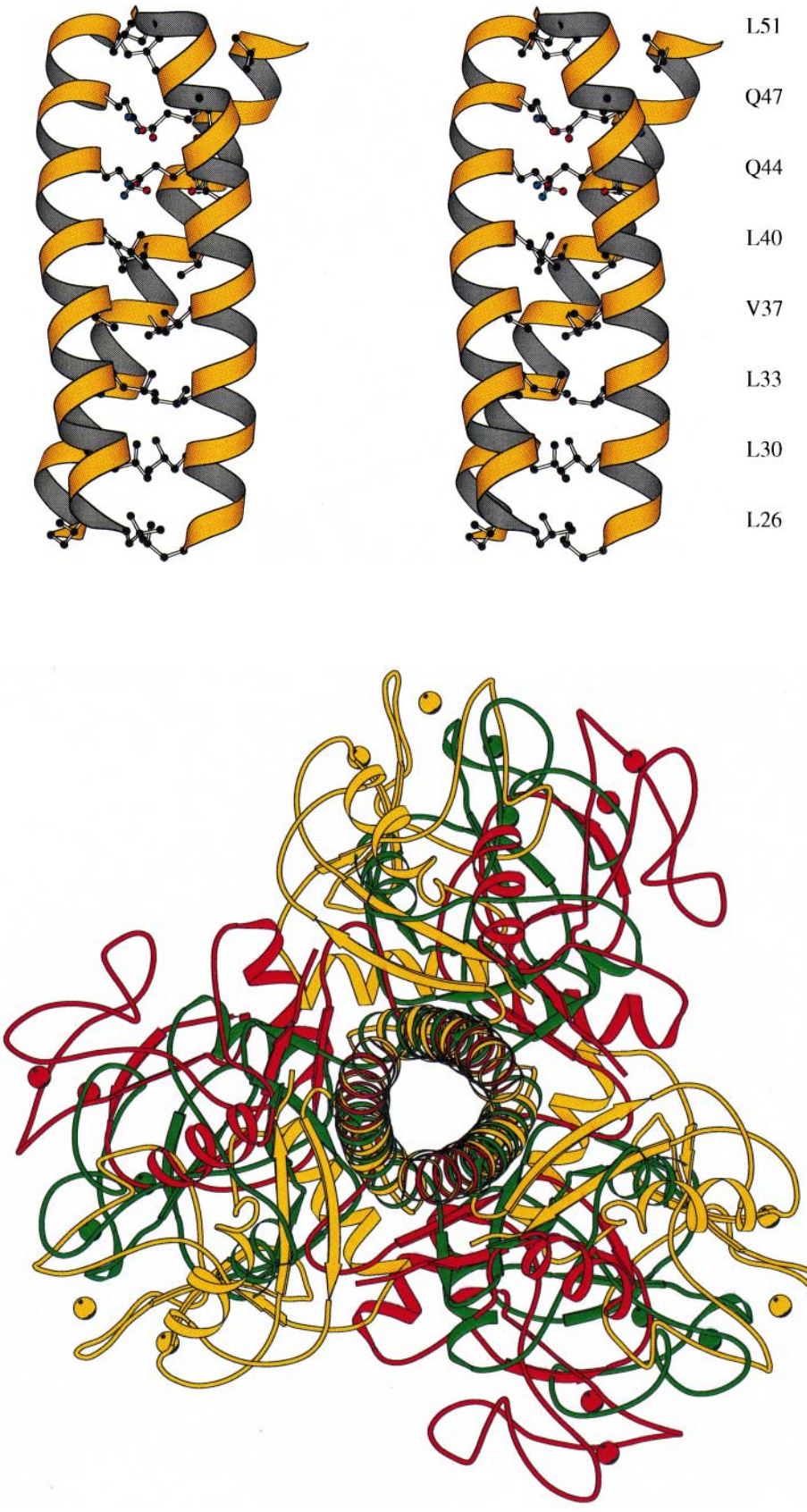

Fig. 2a, b (for caption see page 396).

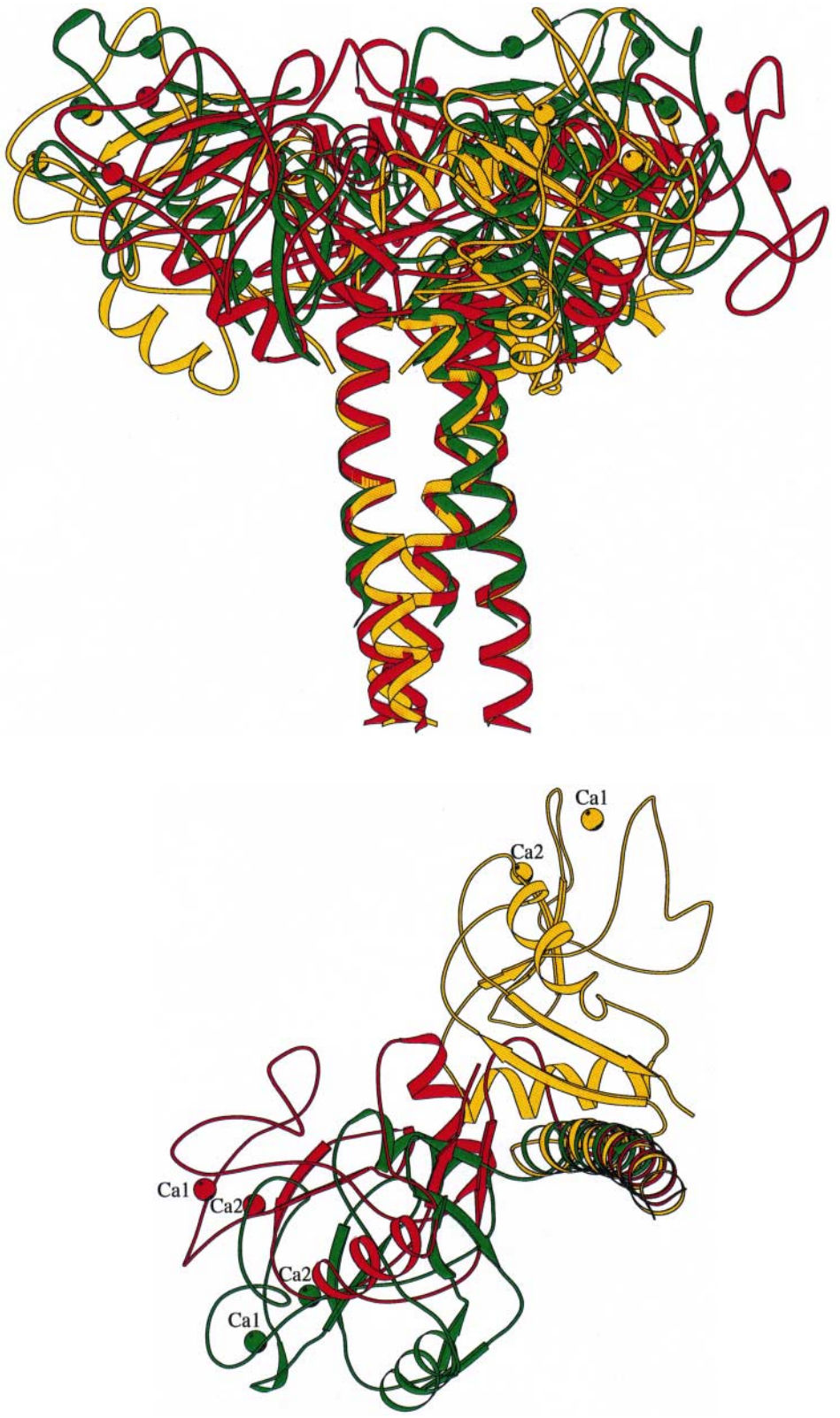

Fig. 2. a: Stereo drawing of the triple α-helical coiled coil of TN viewed perpendicular to the 3-fold axis. The amino acid side chains in **a** and **d** positions of the heptad repeats (Leu^{26}, Leu^{30}, Leu^{33}, Val^{37}, Leu^{40}, Gln^{44}, Gln^{47} and Leu^{51}) are shown in ball and stick. b-c: Superimposition of the helices of the coiled coil in TN (in yellow), in rat MBP from serum (in red) and in human MBP (in green), viewed (c) along and (b) perpendicular to the 3-fold axis. The helices were aligned according to the heptad repeats (Table 2). Calcium ions at site 1 and 2 are illustrated as spheres. d: One monomer of each protein, superimposed as in (b-c), illustrating the relative orientation of the CRDs with respect to the helices. The figures were generated using MOLSCRIPT [39].